

Ising model on hierarchical scale-free networks

Sebastian Komosa* and Janusz A. Hołyst†

Faculty of Physics and Center of Excellence for Complex Systems Research

Warsaw University of Technology

Koszykowa 75, PL-00-662 Warsaw, Poland

(Dated: January 16, 2007)

We studied the behavior of an Ising spin model on different hierarchical scale-free networks using Monte Carlo simulations. We observed a phase transition from ferromagnetism to paramagnetism and a power-law behavior of critical temperature with network size. Two different order parameters were used: a standard average network spin and a weighted network spin. The critical temperature is a power-law function of the ratio $\frac{\langle k^2 \rangle}{\langle k \rangle}$

PACS numbers: 05.80.+q, 89.75.-k, 89.75.Fb

I. INTRODUCTION

To do.

II. MODEL

We considered three models of hierarchical scale-free networks: the first, which is the deterministic, Ravasz-Barabasi (RB) mode [1], the second, the P1 model [2], which is stochastic generalization of the deterministic one, and the next one, the PD model [2], which is a variation of the P1 model.

A. Deterministic model of hierarchical network RB

The starting point is a cluster of five fully connected nodes (a cluster of hierarchy 0). One node in the cluster is the central node. The central node of the cluster is the center of hierarchy 0. Next, we generate four replicas of this first cluster and connect the four external nodes of the replicated clusters to the central node of the first cluster. Now that we have a 25-node module, we again generate four replicas, but this time there are replicas of the 25-node module. Next we connect 16 peripheral nodes of large clusters to the central node of the first cluster, obtaining a new bigger cluster of 125 nodes. We repeat the process until we get a network of a desired hierarchy, as Fig.1.

The growth of a network also starts with a single (cluster of hierarchy 0) with $m + 1$ fully connected nodes, where m is a random number from uniform distribution. One node in a cluster we call center of hierarchy 0. Next we call our cluster the central one and create a random number m of similar clusters. Each one is created in the same way as the central one, but we choose number m

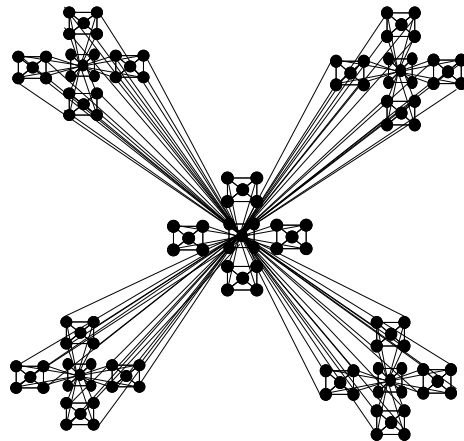


FIG. 1: Network of hierarchy $d = 2$ in RB model.

for every one independently therefore, they may include different numbers of nodes. Next we connect a fraction p of all nodes in non-central clusters to the central node in the central cluster. This node becomes the central node of hierarchy 1. We repeat the process until we get a network of a desired hierarchy fig2.

If we take $P_M(m) = (m, m_0)$, where m_0 is a constant P1 model simplified to the RB model, with a number of nodes and degree distribution determined strictly by p and m_0 . The PD model is a variation of the P1 model, where in each hierarchy d we connect not a part p of nodes but a part p^d .

*Electronic address: seb@if.pw.edu.pl

†Electronic address: jholyst@if.pw.edu.pl

$$X_S = \beta N (\langle S^2 \rangle - \langle S \rangle^2) \quad (4)$$

Where $\langle M \rangle$ and $\langle S \rangle$ are averages over time (100[MCS]).

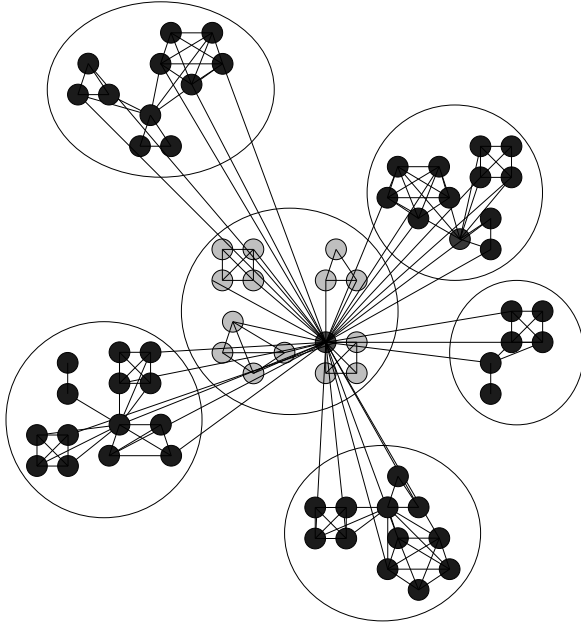


FIG. 2: Network of hierarchy $d = 2$ in P1 model.

B. Simulations

We put every spin $s_i = +1, -1$ on the sites (vertexes) of the network, assumed ferromagnetic coupling between linked spins and a constant coupling strength $J = 1$ and Boltzmann constant $k_B = 1$, where temperature $T = \frac{J}{k_B}$. We conducted standard Monte Carlo simulation with Metropolis Algorithm (average number of time steps for relaxation was between 100 and 200 Monte Carlo time steps [MCS], depending on the size (hierarchy) of the network). During numerical simulations for each hierarchy (size N) of the network, we observed two types of order parameter. The first one was the standard magnetization M of the whole network:

$$M = \frac{1}{N} \sum_{i=1} s_i \quad (1)$$

Where N is a number of vertexes in the network. And the second one was weighted magnetization S :

$$S = \frac{1}{2E} \sum_{i=1} k_i \langle s_i \rangle \quad (2)$$

Where E is a number of links in the network. To investigate a critical temperature T_c of the system for phase transition magnetic susceptibility was observed, respectively, for M (eq.3) and S (eq.4):

$$X_M = \beta N (\langle M^2 \rangle - \langle M \rangle^2) \quad (3)$$

III. NUMERICAL RESULTS

In the ordered network of the given hierarchy d , the temperature T increased. Fig. 3 presents an example of M and S versus T for the P1 model. We observed very similar results for other models (RB, PD).

For low T , we observed very rapid decreases of S and M ,

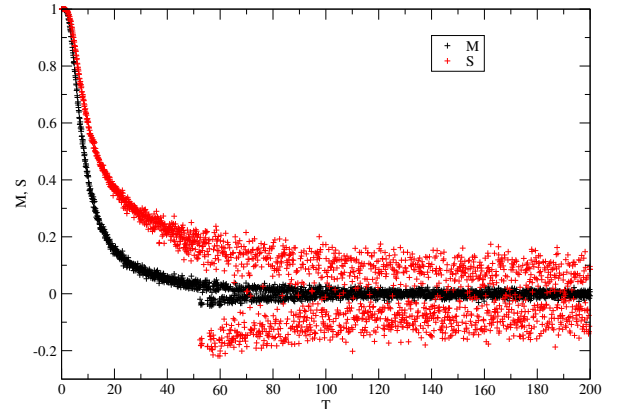


FIG. 3: M (black) and S (red) vs. T , the P1 model, $p=0.7$, for uniform m from 2 to 4, $d=6$ and $N=20000$.

and due to the finite-size effect, it oscillate about zero. The presence of weights in order parameter S (eq. 2) causes higher values because of the high-degree spins. It takes into account that high-degree spin has a bigger impact on S .

To find out the critical temperature of the system, we measured magnetic susceptibility, respectively, for M and S . Fig. 4 shows results for order parameter M and fig.6 shows results for order parameter S (measured in the same P1 network). Similar results we get for the RB and PD models. In fig. 4, we can see the presence of two peaks which cannot be observed in Fig. 6. Weights in S work as a filter, exposing mainly high degree spins fluctuation. Two peaks of magnetic susceptibility in Fig. 4 betray the presence of more than one critical temperature. The first peak in graph of $X_M(T)$ locates the critical temperature for the most weakly connected vertexes (from hierarchy $d = 0, 1$ or 2 , which are 99% of the vertexes of the network). We should observe the spectrum of T_c for each group of vertexes of the given hierarchy, but it is not clearly seen in Fig. 4 because the number of vertexes with higher degree is much lower than the number of vertexes from lower hierarchies and they are not able to create big fluctuation in the system. Only the hub of the whole network has sufficient influence on the network to create a big fluctuation of M during flipping.

Fig. 5 shows magnetic susceptibility X_M^d for each hierarchy from 0 to 7. The fluctuation of X_M^0 near $T = 120$ betrays a strong correlation between hierarchy $d = 0$ and top hierarchies (e.g., hub of the whole network).

Fig. 7 show weighted magnetic susceptibility X_M^d for the each hierarchy from 0 to 7. We observed the highest value of weighted magnetic susceptibility for X_M^7 .

The shapes and tops of the peaks for X_M (the second one) and X_S are not so clear at the first glance. The magnetic susceptibility (eq. 3 and eq. 4) is measured as a size of the thermal fluctuation in the network. The tip shape of the peaks results from fluctuation which appears when with increasing of T (below T_c), the highly connected sites (central node of the network with degree $k \sim p^\gamma * N$) starts flipping. It causes in flipping the network and one big fluctuation appears in the system.

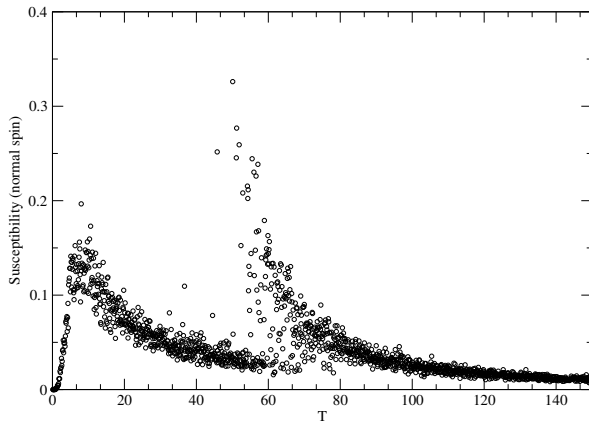


FIG. 4: X_M vs. T for the P1 model, $d = 6, p=0.7$, for uniform m from 2 to 4.

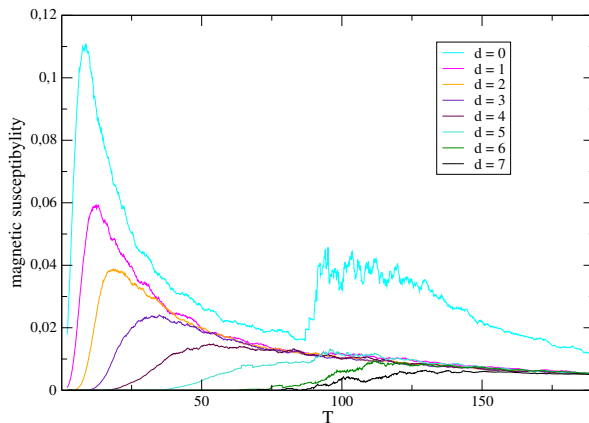


FIG. 5: X_M^d vs. T , spectrum of X_M^d for the given network of the P1 model, $d = 7, p=0.7$, for uniform m from 2 to 4, (avg.=40).

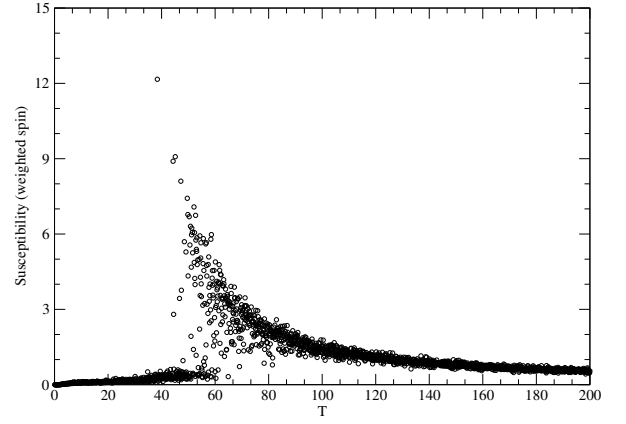


FIG. 6: X_S vs T for P1 model, $d = 6, p=0.7$, for uniform m from 2 to 4.

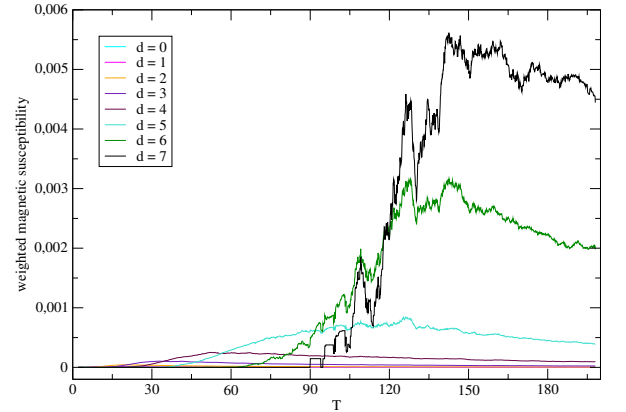


FIG. 7: X_S^d vs. T , spectrum of X_S^d for the given network of the P1 model, $d = 7, p=0.7$, for uniform m from 2 to 4, (avg.=40). For hierarchy $d = 7$ we observed the highest value of weighted magnetic susceptibility.

For further study, we investigated the correlation between all hierarchies. We define this correlation for temperature T as:

$$\xi_{M_{d_i}, d_j} = \frac{\text{cov}(M_{d_i}, M_{d_j})}{\sqrt{\sigma^2(d_i)\sigma^2(d_j)}} \quad (5)$$

where M_{d_i} is define as equ. 1 but concerns only the nodes that belong to hierarchy d_i . Covariance and variance are taken over time $t = 100MCS$. Fig. 8 presents the results for $\xi_{M_{d_i}, d_j}(T)$. We find the biggest value for $\xi_{M_{d_i}, d_j}$, ($db = 07$), when $T \rightarrow T_c^h$ (critical temperature of the main hab). We observe an increas of correlation $\xi_{M_{d_i}, d_j}(T)$ when given hierarchy d_i appraoches its own critical temperature T_c^d (compare with Fig. 5). For lower hierarchies, we observe two peaks at $\xi_{M_{d_i}, d_j}(T)$. When T_c^d is near to T_c^h the influence of fluctuation from the main hub of the network overlaps fluctuation from

hierarchy d , which explains why there is only one peak at $\xi_{M0,d_j}(T)$.

We also investigate the correlation $\xi_{M7,d_j}(T)$ in Fig. 9. We observe the biggest correlation for $db = 70$. Ising models on scale-free networks are systems with a wide spectrum of energy landscape for each subelement (node), with the Boltzman probability for different macroscopic states. We have to stress that it strongly depends on time. Our measurements for $\xi_{M7,d_j}(T)$ were done for $t = 100[MCS]$. For very long period of observation, we should expect a full correlation $\xi_{M7,d_j}(T) \rightarrow 1$ for $0 < T < T_c^h$.

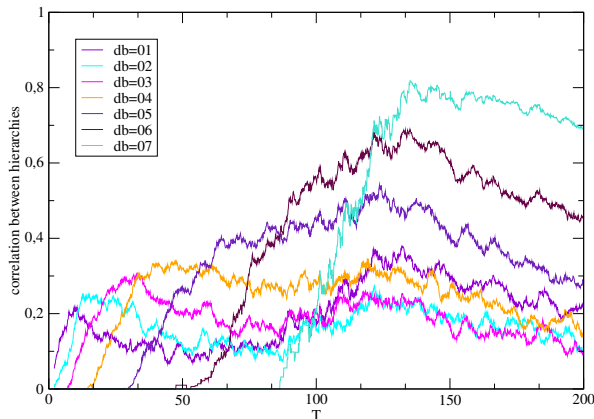


FIG. 8: $\xi_{M(0,d_j)}$ vs. T , correlation between hierarchies 0 and d_j ($db = 0d_j$) in the P1 model, $d = 7$, $p=0.7$, for uniform m from 2 to 4, (avg.=40). The strongest correlation between hierarchy $d = 0$ and $d = 7$ (the main hub of the network).

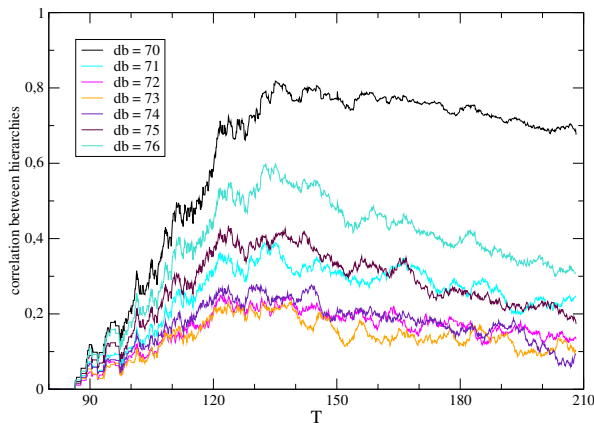


FIG. 9: $\xi_{M(7,d_j)}$ vs. T , correlation between hierarchies 7 and d_j ($db = 7d_j$) in the P1 model, $d = 7$, $p=0.7$, for uniform m from 2 to 4, (avg.=40). The strongest correlation between hierarchy $d = 0$ and $d = 7$ (the main hub of the network).

For every hierarchical model for each hierarchy d starting from $d = 2$, we measured X_M and X_S . From binned magnetic susceptibility data, we get T_c versus the size of network N . For every hierarchical model, we find out power-law behavior $T_c \sim N^\gamma$. Fig. 10 presents the results for order parameter M and Fig. 11 presents the results for S . In Fig. 12 we compare the results from Figs. 10 and 11. The difference in Fig. 12 derives from fitting errors.

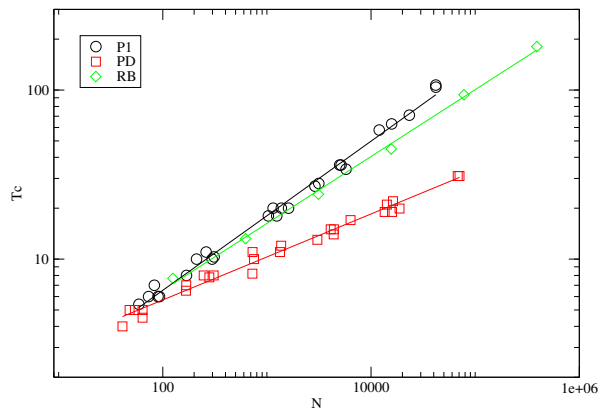


FIG. 10: T_c vs. N for order parameter M , data (points) and fitted results (solid lines); the P1 model, $p=0.7$, for uniform m from 2 to 4, from fitting $\gamma_{P1} = 0.44$; the PD model, $p=0.7$, for uniform m from 2 to 4, from fitting $\gamma_{PD} = 0.25$; and RB model, from fitting $\gamma_{RB} = 0.4$.

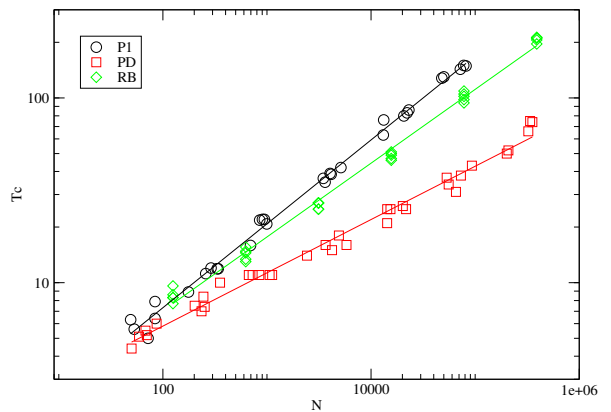


FIG. 11: T_c vs N for order parameter S , data(points) and fitted results (solid lines); the PD model, $p=0.7$, for uniform m from 2 to 4, from fitting $\gamma_{P1} = 0.45$; the PD model, $p=0.7$, for uniform m from 2 to 4, from fitting $\gamma_{PD} = 0.28$; and RB model, from fitting $\gamma_{RB} = 0.38$.

In [5] Bianconi introduced mean field approximation with weighted spin (eq. 2) (MFAWS) for random network (Barabasi-Albert) as relationship eq. 6. After

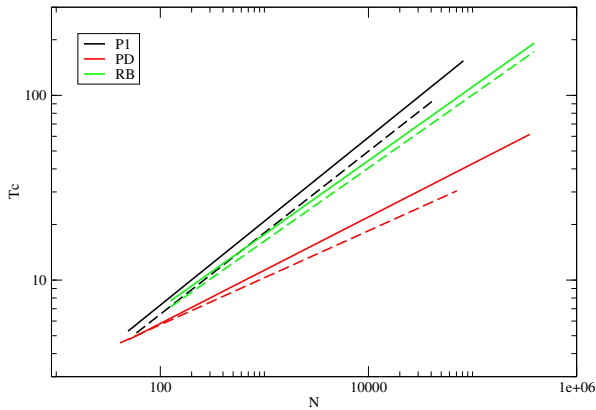


FIG. 12: T_c vs N , for the hierarchical models; P1 (black), PD (red) and RB (green), with order parameter M (solid lines) and S (discontinuous lines).

simple algebra, we get eq. 7, where $\beta = 1/T$ and h_i is external field acting on spin i . With this assumption and taking $\beta = \beta_c$ we get the effective critical temperature which is $T_c \sim \ln(N) \sim \frac{\langle k^2 \rangle}{\langle k \rangle}$ (solution for BA model in eq. 8).

$$\langle s_i \rangle = \tanh[\beta(Jk_i S + h_i)] \quad (6)$$

$$S = \frac{1}{2E} \sum_{i=1} k_i \tanh[\beta(Jk_i S + h_i)] \quad (7)$$

$$\frac{T_c}{J} = \frac{m}{2} \ln(N) \sim \frac{\langle k^2 \rangle}{\langle k \rangle} \quad (8)$$

Because our numerical results don't satisfy the Bianconi solution ($T_c \sim \ln(N)$), we investigated the relationship eq. 6 on hierarchical models. Figs. 13, 14, and 15 present the results for two order parameters with $T < T_c$, respectively, for each hierarchical model. The two order parameters take effect in shift values at the x-axis.

In Fig. 13, the P1 model has the best compatibility with MFAWS (eq. 6), spins with few neighbor flips, when those with many neighbors point to one state most of the time. In the PD model (Fig. 14) we observed incompatibility with MFAWS, spins with an average number of neighbors flips most often when spins with few and many neighbors stay in one state. In the PD model in each hierarchy d we connect a part p^d of new nodes. The PD model has a lower density of links in network than the P1 model. It produces clusters in the network, which have opposite magnetization than the rest of the network, which is what causes incompatibility with MFAWS. The RB model is fully deterministic; it is a particular case of the P1 and PD models when we take the distribution of

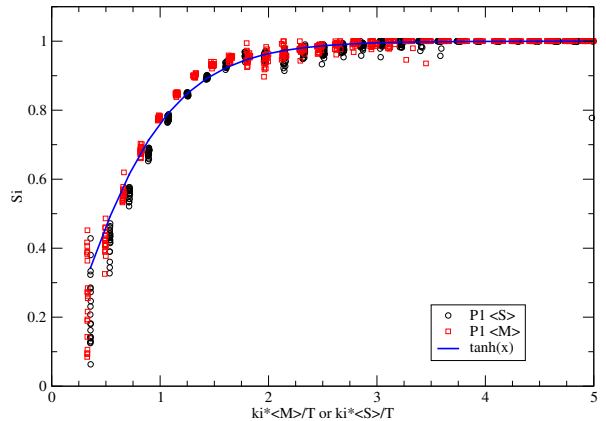


FIG. 13: Results for the P1 model, $d = 7$, $p=0.7$, for uniform m from 2 to 4, measured $\langle s_i \rangle$ of site i versus $k_i \beta M$ (red points) or $k_i \beta S$ (black points) in $T = 5$, mean field prediction $\tanh(x)$ (solid line), results over 20 networks respective for each order parameter.

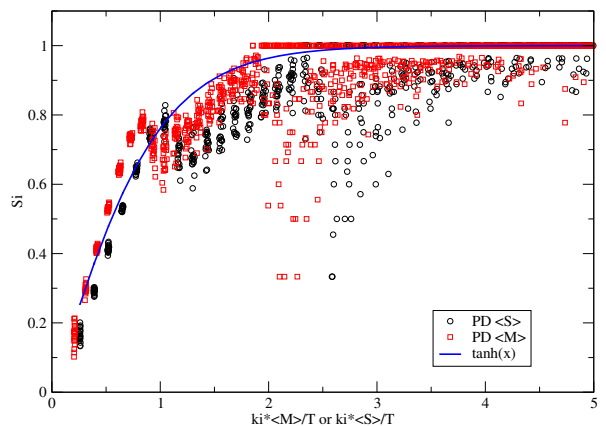


FIG. 14: Results for the PD model, $d = 7$, $p=0.7$, for uniform m from 2 to 4, measured $\langle s_i \rangle$ of site i versus $k_i \beta M$ (red points) or $k_i \beta S$ (black points) in $T = 5$, mean field prediction $\tanh(x)$ (solid line), results over 20 networks respective for each order parameter.

m as $\delta(m, m_0)$ (m_0 is constant) and a special way of linking new nodes. In Fig. 15, we observed similar behavior as for the PD model.

In [5] Bianconi showed that for random networks relationship $T_c \sim \frac{\langle k^2 \rangle}{\langle k \rangle}$ is fulfilled. Fig. 16 presents the results for the hierarchical networks (P1, PD, RB). During the simulations, we measured for each network at once T_c (from $X_S(T)$) and $\frac{\langle k^2 \rangle}{\langle k \rangle}$, respectively, each hierarchical model. We find power-law dependence

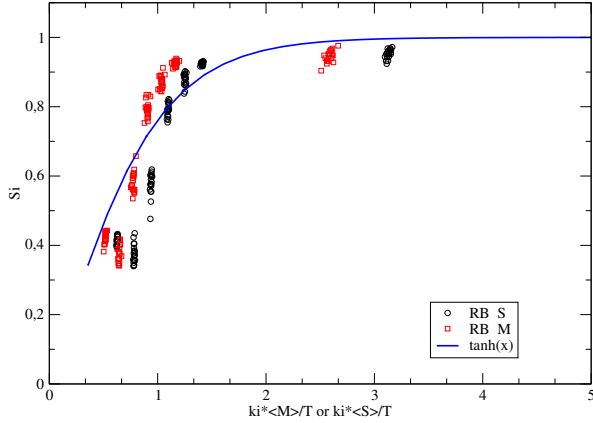


FIG. 15: Results for the RB model, $d = 7$, measured $\langle s_i \rangle$ of site i versus $k_i \beta M$ (red points) or $k_i \beta S$ (black points) in $T = 5$, mean field prediction $\tanh(x)$ (solid line), results over 20 networks respective for each order parameter.

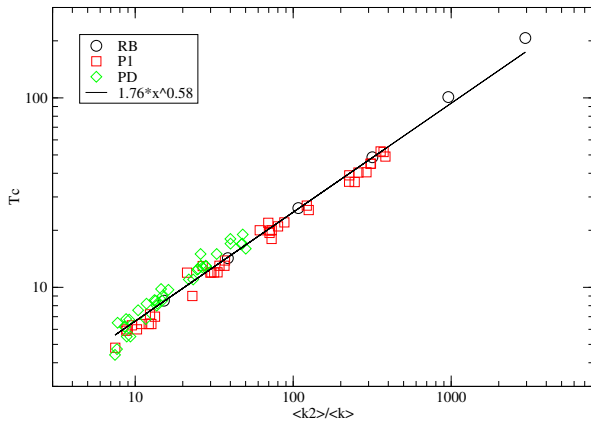


FIG. 16: Results T_c vs. $\frac{\langle k^2 \rangle}{\langle k \rangle}$ for the P1 model (red squares), $p=0.7$, for uniform m from 2 to 4, for the PD model (green diamonds), $p=0.7$, for uniform m from 2 to 4 and the RB model (black circles), fitted data (P1, PD, RB) (black solid line) $\alpha = 0.58$.

$T_c \sim \left(\frac{\langle k^2 \rangle}{\langle k \rangle}\right)^\alpha$ for all hierarchical models (P1, PD, RB), from fitting $\alpha = 0.58$.

For more statistical analysis, the relationship $\frac{\langle k^2 \rangle}{\langle k \rangle}$ with N was observed. During simulations, we measured for each network at once $\frac{\langle k^2 \rangle}{\langle k \rangle}$ and N , respectively, each hierarchical model (P1, PD, RB). Fig. 17 presents the power-law behavior $\frac{\langle k^2 \rangle}{\langle k \rangle} \sim N^\mu$.

In the system for $T \ll T_c$ we flip one spin and left

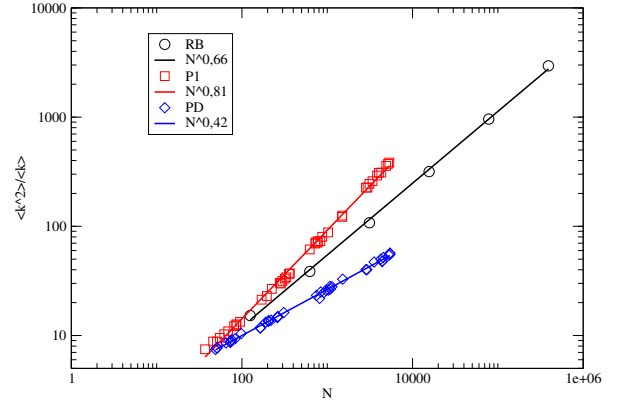


FIG. 17: $\frac{\langle k^2 \rangle}{\langle k \rangle}$ versus N for the P1, PD, and RB models, from fitting $\mu_{P1} = 0.81$, $\mu_{PD} = 0.42$ and $\mu_{RB} = 0.66$.

it in the new unchangeable state; this procedure we call *pinning*. Pinning one spin in mean field approximation might be seen as introducing an external field in the system acting oppositely at its neighbors. During simulations in the ordered network, we started the pinning procedure from the site with the highest degree and repeated the procedure for the site with the next highest degree. Continuing pinning in the system, we measured M . After a few steps, the whole network reached opposite polarization, and continued phase transition in the system can be observed. Fig. 18 presents the results for the P1 model with average $\langle m \rangle = 4.5$. It is enough to pin the center of the network (the main hub of the network) and the centers of neighbor clusters to reach opposite polarization. We get similar results for the PD and RB models.

For further study, the pinning procedure was changed. During the simulation when $M = M_0$, we stopped the pinning procedure and released the pinned spins. Fig. 19 and fig. 20 shows the results for the P1 model. We get similar results for the PD and RB models. After releasing the pinning, system reaches the stable state. These observations can be explained by the structure of the network; the small density of connection of the clusters results in weak coupling between big parts of the network, and a cluster with opposite polarization from the rest of the network appears.

IV. CONCLUSIONS

To do.

Acknowledgments

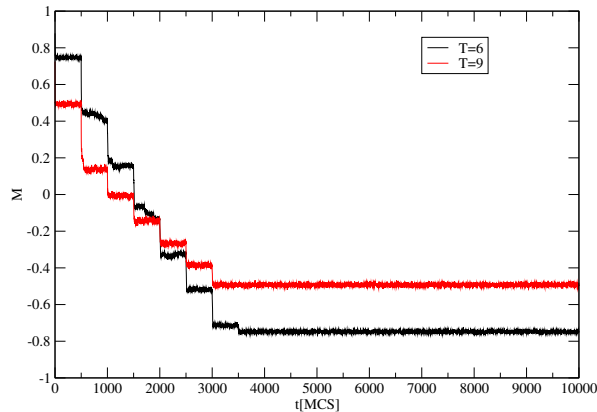


FIG. 18: Pinning procedure for the P1 model, $d = 5$, $p = 0.7$, for uniform m from 2 to 4. Results for $T = 6$ (black) and $T = 9$ (red). Phase transition after flip 5 highly connected nodes.

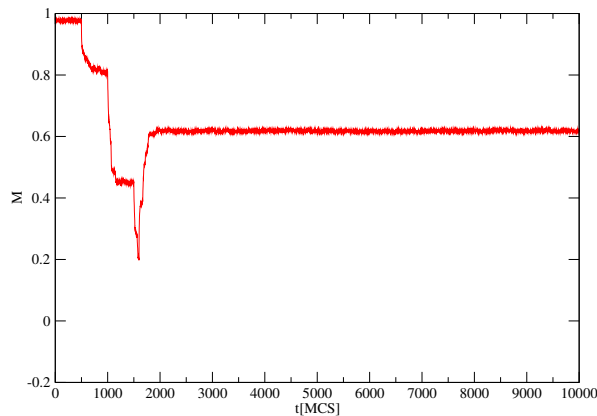


FIG. 19: Pinning procedure with resetting at $M = 0.2$ for the P1 model, $d = 5$, $p = 0.7$, for uniform m from 2 to 4. Results for $T = 3$.

This work was partially supported by an EU Grant *Measuring and Modelling Complex Networks Across Domains* (MMCOMNET) and by an EU Grant *Critical events in evolving networks* (CREEN) (Grant No.012864).

-
- [1] E.Ravasz, A.-L.Barabási, Phys. Rev. E **67**, 026112 (2003).
 [2] K. Suchecki, J.A. Hoyst, A.P.P. B **36(8)**, 2499-2511 (2005)
 [3] A.-L. Barabasi, R. Albert, Science **286**, 509 (1999).
 [4] A. Aleksiejuk, J.A. Holyst, D. Stauffer, Physica A **310**, 260-266 (2002).
 [5] G. Bianconi, Phys. Lett. A **303** (2002), 166-168.
 [6] S.N. Dorogovtsev, A.V. Goltsev, J.F.F. Mendes, Phys. Rev. E **66**, 016104 (2002).
 [7] A.V. Goltsev, S.N. Dorogovtsev, J.F.F. Mendes, Phys. Rev. E **67**, 026123 (2003).
 [8] C.P. Herrero, Phys. Rev. E **69**, 067109 (2004).
 [9] B. Tadic, K. Malarz, K. Kulakowski, Phys. Rev. Lett. **94**, 137204 (2005).
 [10] M.A. Sumour, M.M. Shabat, Int. J. Mod. Phys. C **16**, 585-589 (2005).
 [11] D.H. Kim, G.J. Rodgers, B. Kahng, D. Kim, Phys. Rev. E **71**, 056115 (2005).
 [12] J.A. Holyst, K. Kacperski, F. Schweitzer, Physica A **285**, 199-210 (2000).
 [13] J.A. Holyst, K. Kacperski, F. Schweitzer, Annual Review of Comput. Phys. **9**, 253-273 (2001).
 [14] S. Galam, J. Applied Physics **87**, 7040-7042 (2000).
 [15] M. Lewenstein, A. Nowak, B. Latane, Phys. Rev. A **45**, 763 (1992).
 [16] M. Girvan, M.E.J. Newman, Proc. Natl. Acad. Sci. USA **99**, 7821-7826 (2002).

- [17] D.F. Zheng, G. Ergun, *Adv. Complex Systems* **6**, 507-514 (2003).
- [18] D. Chowdhury, D. Stauffer, *Principles of Equilibrium Statistical Mechanics* (Wiley-VCH, Berlin, 2000).

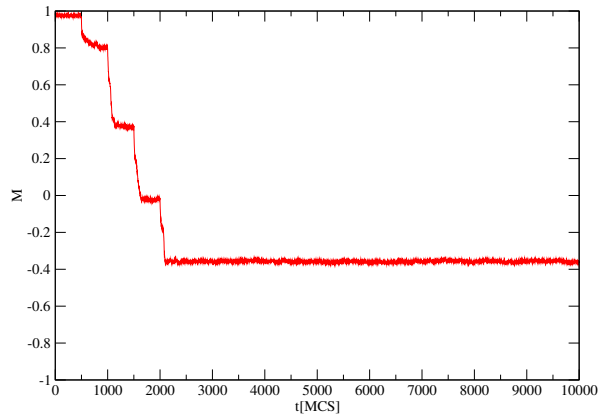


FIG. 20: Pinning procedure with resetting at $M = -0.2$ for the P1 model, $d = 5$, $p = 0.7$, for uniform m from 2 to 4. Results for $T = 3$.